Published in final edited form as:
J Biomech. 2013 November 15; 46(16): 2787–2794. doi:10.1016/j.jbiomech.2013.09.003.

Fiber micro-architecture in the longitudinal-radial and circumferential-radial planes of ascending thoracic aortic aneurysm media

Alkiviadis Tsamis[a,d,f], **Julie A. Phillippi**[a,b,d,f], **Ryan G. Koch**[a], **Salvatore Pasta**[g,h], **Antonio D'Amore**[f,g,h], **Simon C. Watkins**[e], **William R. Wagner**[a,b,d,f], **Thomas G. Gleason**[a,b,d,f], and **David A. Vorp**[a,b,c,d,f,*]

David A. Vorp: vorp@pitt.edu

[a]Department of Bioengineering, University of Pittsburgh, Pittsburgh, PA, United States

[b]Department of Cardiothoracic Surgery, University of Pittsburgh, Pittsburgh, PA, United States

[c]Department of Surgery, University of Pittsburgh, Pittsburgh, PA, United States

[d]Center for Vascular Remodeling and Regeneration, University of Pittsburgh, Pittsburgh, PA, United States

[e]Center for Biologic Imaging, University of Pittsburgh, Pittsburgh, PA, United States

[f]McGowan Institute for Regenerative Medicine, University of Pittsburgh, Pittsburgh, PA, United States

[g]Fondazione Ri.MED, Palermo, Italy

[h]DICGM University of Palermo, Palermo, Italy

Abstract

It was recently demonstrated by our group that the delamination strength of ascending thoracic aortic aneurysms (ATAA) was lower than that of control (CTRL, non-aneurysmal) ascending thoracic aorta (ATA), and the reduced strength was more pronounced among bicuspid (BAV) vs. tricuspid aortic valve (TAV) patients, suggesting a different risk of aortic dissection for BAV patients. We hypothesized that aortic valve morphologic phenotype predicts fiber micro-architectural anomalies in ATA. To test the hypothesis, we characterized the micro-architecture in the longitudinal-radial (Z-RAD) and circumferential-radial (Θ-RAD) planes of human ATA tissue that was artificially dissected medially. The outer and inner-media of CTRL-ATA, BAV-ATAA and TAV-ATAA were imaged using multi-photon microscopy in the Z-RAD and Θ-RAD planes to observe collagen and elastin. Micrographs were processed using an image-based tool to quantify several micro-architectural characteristics. In the outer-media of BAV-ATAA, elastin was more undulated and less aligned about the Θ-axis when compared with CTRL-ATA, which is consistent with increased tensile stretch at inflection point of Θ-strips of adventitial-medial half of BAV-ATAA (1.28) when compared with CTRL-ATA (1.13). With increasing age, collagen became more undulated about the *Z*-axis within the outer-media of TAV-ATAA, and elastin

*Corresponding author at: Swanson School of Engineering, University of Pittsburgh, 123 Benedum Hall, 3700 O'Hara Street, Pittsburgh, PA 15261, United States. Tel.: +1 412 624 8503; fax: +1 412 624 0412.

Appendix A. Supplementary material: Supplementary data associated with this article can be found in the online version at http://dx.doi.org/10.1016/j.jbiomech.2013.09.003.

Conflict of interest statement: The authors do not have any financial interest or other relationship (grant, research support, consultant, etc.) with any manufacturer(s) of any commercial product(s) to disclose.

became more oriented in the *Z*-axis and collagen less radially-oriented within the inner-media of TAV-ATAA. This discrepancy in the micro-architecture with fibers in the inner layers being more stretched and with disrupted radially-oriented components than fibers in the outer layers may be associated with the development, progression and vascular remodeling in aneurysms arising in TAV patients.

Keywords

Human ascending thoracic aortic aneurysm; Elastin; Collagen; Micro-architecture; Multi-photon microscopy; Dissection

1. Introduction

Ascending aortic disease manifesting as aneurysm or dissection is currently a major health concern (Jondeau and Boileau, 2012; Lu et al., 2012; Matsushita et al., 2012; Takigawa et al., 2012). Aortic dissection (AoD) usually begins with an intimal tear in the thoracic aorta, which permits blood to enter the wall, split the media and create a false lumen that can reenter the true lumen anywhere along the course of AoD or exit through the adventitia causing complete rupture (Lu et al., 2012; Matsushita et al., 2012). AoDs are classified in different types (DeBakey I, II, III and Stanford A, B), and those which involve the ascending thoracic aorta (ATA) are considered a cardiovascular emergency with an extraordinarily high lethality (Masuda et al., 1991).

From a biomechanics standpoint, a possible mechanism for dissection is that blood pressure-induced stresses exceed the adhesive strength that holds the elastic layers of ATA together. We recently quantified the adhesive strength (resistance to delamination (S_d) of aortic layers) in both non-aneurysmal and aneurysmal human ATA among patients with bicuspid aortic valve (BAV) and tricuspid aortic valve (TAV). This was accomplished by artificially dissecting the ATA specimens medially by means of delamination testing (Pasta et al., 2012). The S_d of ascending thoracic aortic aneurysm (ATAA) was lower irrespective of aortic valve morphology ($S_{d,Z}$=100 mN/mm and $S_{d,\Theta}$ =88 mN/mm for BAV-ATAA, and $S_{d,Z}$ =117 mN/mm and $S_{d,\Theta}$=109 mN/mm for TAV-ATAA) when compared to control (CTRL)–ATA ($S_{d,Z}$=149 mN/mm and $S_{d,\Theta}$ =126 mN/mm) in either longitudinal (Z) or circumferential (Θ) direction. The lower S_d of BAV-ATAA compared to TAV-ATAA suggested that the former has an apparent increased risk of AoD.

The S_d of aorta may be altered by the nature of local micro-architecture, mainly characterized by the transmural content and orientation of both elastin and collagen fibers. Specifically, S_d may be affected by the interlaminar elastin and collagen fibers and especially those fibers which are radially-oriented. The latter contribute to the adhesive cell-matrix forces that hold the aortic layers together. Therefore, in the degenerated ATAA wall (de Figueiredo Borges et al., 2008), the forces developed by hemodynamics may exceed the adhesive forces holding the mural layers together, likely inducing spontaneous tears in the weakened aorta as suggested by Pasta et al. (2012). We recently uncovered distinct patterns of aortic medial matrix remodeling in BAV compared to TAV patients and demonstrated a more highly-aligned collagen and elastin micro-architecture pattern in the Θ–Z plane (Phillippi et al., in press) in accordance with our observations of increased tensile strength in BAV-ATAA when compared with TAV-ATAA (Pichamuthu et al., in press).

Collectively, these data suggested that aortic valve morphologic phenotype correlates with predictable changes in fiber micro-architecture of ATA. To test the hypothesis, we characterized the collagen and elastin micro-architecture in the tunica media in the

longitudinal-radial (Z-RAD) and Θ-RAD planes of BAV-ATAA, TAV-ATAA and CTRL-ATA, assuming that the lower S_d of BAV-ATAA is related to differences in fiber micro-architecture of the investigated tissue planes. The data suggest that the architecture of radially-oriented fibers correlates with aortic valve morphology.

2. Methods

2.1. Human aorta specimens

All the collected human ATA specimens were gathered from our previous experimental study (Pasta et al., 2012) according to guidelines of our Institutional Review Board and Center for Organ Recovery and Education. Segments of CTRL-(non-aneurysmal)-ATAs were collected from organ donor/recipient subjects with TAV, whereas non-dissected ATAAs were obtained fresh from patients with either BAV or TAV undergoing elective repair of aneurysmal aorta at the University of Pittsburgh Medical Center. From the original study (Pasta et al., 2012), we analyzed a subset of artificially dissected *Z* and Θ-strips which were not subjected to tensile testing of delaminated halves up to failure. Both adventitial-medial and medial-intimal delaminated halves from 5 CTRL-ATAs, 8 BAV-ATAAs and 5 TAV-ATAAs from patients with age ranging 39–81 years and aortic diameter 46–68 mm (8 men and 10 women) were perfusion-fixed in 4% paraformaldehyde. After replacement of the solution with phosphate buffered saline (i.e. approximately after 1.5 h), the specimens were stored at 4°C and designated for state-of-the-art multi-photon microscopy for evaluating the fiber micro-architecture. Table 1 summarizes patient demographic data of each ATA sample.

2.2. Multi-photon microscopy

Imaging analyses were performed using an Olympus multi-photon microscope (Model FV10, ASW software) to observe elastin and collagen fiber arrangement in the *Z*-RAD and Θ-RAD planes of ATA samples (Fig. 1) (Cahalan et al., 2002; Jiang et al., 2011; Konig et al., 2005). During imaging, the *Z*-RAD or Θ-RAD planes of both adventitial-medial and medial-intimal delaminated halves from $\boldsymbol{\Theta}$ (Fig. 1, illustrated in column 1) and *Z*-strips (Fig. 1, illustrated in column 4) faced the microscope lens to allow for visualization of radially-oriented collagen and elastin fibers. Elastin (green) and collagen (red) fibers were automatically detected according to intrinsic fluorescence (channel RXD1, wavelength=525 ±25 nm) and second harmonic generation (channel RXD2, wavelength=400 ± 50 nm), respectively.

2.3. Image-based analysis to assess wall micro-architecture

A custom automated image-based analysis tool developed in MATLAB (Math-Works, Inc., R2011a) based on image background removal (D'Amore et al., 2010) and on fiber detection algorithm (Karlon et al., 1998) was used to process the multi-photon images showing collagen and elastin fiber network in both *Z*-RAD and Θ-RAD planes of BAV-ATAA, TAV-ATAA and CTRL-ATA. Multi-photon images were taken within 500 (μm above and 500 (μm below the dissected medial surface (Fig. 1, rows 2-3), which are denoted as outer-media and inner-media, respectively. Fig. 2 displays a representative multi-photon image (0.5×0.5 mm^2) of collagen fibers in the outer-media of TAV-ATAA in the *Z*-RAD plane (Fig. 2A) and the output generated by the image-based analysis tool (Fig. 2B,C,F). The scripts first generate small arrows (white) that follow the fiber direction (Fig. 2B). Each of these arrows has an individual orientation, with 90° denoting *Z*-orientation (or Θ-orientation if the image belongs to Θ-RAD plane) and 0° or 180° denoting RAD-orientation toward either intima or adventitia, respectively. The algorithm also is able to filter the fiber components with a *Z* or RAD-orientation using a small angle tolerance of 5° as shown in Fig. 2D, and provides the corresponding % of fibers oriented in the RAD or *Z*-direction. Fig.

2C shows the processed image with the radially-oriented fiber segments overlaid in red color.

The fiber angle distribution (counts vs. angle) was then plotted as shown in Fig. 2F. The left and right peak of the histogram corresponds to a dominant angle which is lower and higher than the mean angle of orientation, respectively. The angle difference between the two peaks represents the average amplitude of fiber angular undulation (AAU) about the *Z*-axis as graphically explained in Fig. 2G. Fig. 2F also indicates the parts of the histogram that correspond to fibers oriented in the *Z* and RAD-direction.

Finally, the script quantifies the fiber orientation index (*OI*), which provides a measure of fiber alignment (D'Amore et al., 2010). The *OI* is calculated as

$$OI = (1/\mathrm{n}) \sum \cos^2(\theta_i), \quad (1)$$

where θ_i is the angle of a fiber segment $i = 1 \ldots n$ with respect to the direction of supposed alignment. The latter can be chosen as the mean angle of fiber orientation (Fig. 2F). An *OI*=1 indicates a perfectly aligned fiber set in a preferred direction or anisotropy, while *OI*=0.5 indicates random fiber alignment or isotropy.

2.4. Statistical analysis

One-way ANOVA ($p < 0.05$) followed by Tukey post-hoc test (unequal samples) for all pair-wise comparisons was performed using SigmaPlot software (SYSTAT Software, Chicago, Ill) to determine significant differences in collagen and elastin micro-architecture among groups (BAV-ATAA *n* =8, TAV-ATAA *n*=5, CTRL-ATA *n*=5) in the outer-media and inner-media of *Θ*-RAD and *Z*-RAD planes. Data are presented as mean ± standard error mean. Linear regression analysis was performed to study correlation with patient demographic data (i.e. aneurysm diameter and patient age).

3. Results

3.1. Morphometric assessment of ATA in transverse planes

3.1.1. Observations of the Z-RAD plane—Multi-photon images revealed that both collagen and elastin fibers in the *Z*-RAD plane of outer-media were almost parallel with each other and were less numerous, more undulated about the *Z*-axis, and less dense in ATAA, when compared with CTRL-ATA (Fig. 1, row 2, columns 2–4, see also Figs. S1 and S2). Similarly, the collagen and elastin fibers also appeared to be parallel with each other in the *Z*-RAD plane of inner-media, but their density was the same in aneurysmal and CTRL-ATA (Fig. 1, row 3, columns 2–4). The fibers appeared less undulated about the *Z*-axis in TAV-ATAA than in BAV-ATAA.

3.1.2. Observations of the Θ-RAD plane—In the *Θ*-RAD plane of outer-media, parallel collagen and elastin fibers were less in number, more undulated about the *Θ*-axis and less dense in ATAA when compared with CTRL-ATA (Fig. 1, row 2, columns 6–8). The density and undulation of the fibers were similar in BAV and TAV-ATAA. Similarly, in the *Θ*-RAD plane of inner-media, the fiber arrangement was less dense and fibers were more undulated about the *Θ*-axis in ATAA compared to CTRL-ATA (Fig. 1, row 3, columns 6–8). The density of the fibers was similar between BAV and TAV-ATAA. However, fibers were found to be less undulated about the *Θ*-axis in BAV-ATAA than in TAV-ATAA.

3.1.3. Overall observations—The qualitative visual assessment revealed that the fiber micro-architecture in the outer-media is similar in the *Z*-RAD and *Θ*-RAD planes, with fibers being less dense in ATAA when compared with CTRL-ATA. In the inner-media, fibers seem to be less undulated about the *Θ*-axis in BAV-ATAA when compared with TAV-ATAA, which may contribute to reduced ability of inner-media layers of BAV-ATAA to resist to radial loads. The statistical analyses provided quantitative results for the fiber micro-architecture in the various tissue planes among patients grouped by valve phenotype.

3.2. Quantitative comparison among ATA phenotypes

Statistical analysis of the images which were taken within 500 μm above and 500 μm below the dissected medial surface showed that, in the *Θ*-RAD plane in the outer-media, elastin fibers seemed to be more undulated about *Θ*-axis, less aligned in the *Θ*-axis, and less oriented about the *Θ*-direction in the BAV-ATAA when compared with CTRL-ATA. This was indicated by a higher AAU (Fig. 3A), lower *OI* (Fig. 3B), and lower *Θ*% of elastin fibers (Fig. 3C), respectively, in BAV-ATAA when compared with CTRL-ATA. The ratio RAD/*Θ* was also higher in BAV-ATAA for both elastin (Fig. 3D) and collagen fibers (Fig. 3E) when compared to CTRL-ATA. Overall, we observed a tendency for both elastin and collagen fibers to be more radially-oriented in the outer-media of BAV-ATAA when compared with CTRL-ATA, that may contribute to improved radial strength of outer-media in BAV-ATAA.

3.3. Effect of aneurysm diameter and age on fiber micro-architecture

Linear regression analysis of imaging data taken within 500 μm above and 500 μm below the dissected medial surface revealed that with increased aneurysm diameter, collagen fibers in the inner-media of TAV-ATAA seemed to become less radially-oriented and more *Θ*-oriented. This was indicated by a decreasing ratio RAD/*Θ* (Figs. 4A, R=0.9522), decreasing RAD% (Fig. 4B, R=0.9580), increasing *OI* (Fig. 4C, R=0.9766) and increasing *Θ*% (Fig. 4D, R=0.9653). With increased patient age, collagen fibers were found to be more undulated about the *Z*-axis in the outer-media of TAV-ATAA, and this was indicated by an age-related increase in AAU of collagen (Fig. 4E, R=0.8901). However, in the inner-media of TAV-ATAA, elastin fibers were observed to be more Z-oriented and collagen fibers were less radially-oriented with increasing age, as shown by an age-associated increase in *Z*% of elastin (Fig. 4F, R=0.8853) and decrease in RAD% of collagen (Fig. 4G, R=0.9218), respectively. Results show that the aneurysm diameter and patient age seemed to influence fiber micro-architecture of TAV-ATAA only. Interestingly, with increasing patient age, fibers in the outer-media of TAV-ATAA became more undulated about the *Z*-axis, i.e. more radially-oriented, whereas fibers in the inner-media of TAV-ATAA became less radially-oriented, which may compromise the radial strength of inner-media in TAV-ATAA.

4. Discussion

4.1. Interpretation of morphometric examination

Qualitative assessment of multi-photon imaging near the dissected medial surface revealed that the outer-media exhibited fibers which seemed to be more undulated about the *Z*-axis in BAV compared to TAV-ATAA (Fig. 1, row 2, also see Figs. S1-S2). However, within the inner-media, fibers seemed to be more undulated about *Z*-axis in BAV-ATAA, compared to TAV-ATAA and CTRL-ATA (Fig. 1, row 3). In the *Θ*-RAD plane, fibers were generally less undulated about *Θ*-axis in BAV compared to TAV-ATAA in the inner-media. The reduced undulation of fibers about *Θ*-axis in the inner-media of BAV-ATAA relative to TAV-ATAA may compromise the ability of inner-media layers of BAV-ATAA to resist to radial loads and predispose to inner-media micro-tears in BAV-ATAA.

Overall, both collagen and elastin fibers were less numerous, parallel with each other, and less dense in ATAA than CTRL-ATA in both Z-RAD and Θ-RAD planes, suggesting an altered microstructure in ATAA which could be associated with vascular remodeling in aneurysms. Borges et al. demonstrated prominent elastin lamellae, which were also interconnected by a network of small interlaminar elastin and collagen fibers in CTRL-ATA (de Figueiredo Borges et al., 2008; Nakashima et al., 1990a; Sariola et al., 1986). These lamellae were not easily identified in ATAA samples in this study (Fig. 1 rows 2,3 columns 2,3,6,7), but could contribute increased S_d between wall layers.

4.2. Aortic architectural comparison among valve morphologic phenotypes

We recently reported a more highly-aligned collagen and elastin fiber micro-architecture in BAV-ATAA specimens compared to TAV-ATAA and CTRL-ATA, and these differences were associated with altered collagen maturity (Phillippi et al., 2013). These observations were made of the aortic media en face (i.e. Θ-Z plane) and indicated that different mechanisms of vascular remodeling are at play in BAV and TAV patients. This current study documents the collagen and elastin fiber micro-architecture in the other two planes (i.e. Θ-RAD and Z-RAD). Increased undulation of elastin fibers about the Θ-axis (Fig. 3A B) and increased amount of radially-oriented elastin and collagen fiber components (Fig. 3C and E) was noted in the outer-media of BAV-ATAA compared to CTRL-ATA which was not appreciated in TAV-ATAA. This finding is compatible with increased tensile stretch at the inflection point of Θ-strips of adventitial-medial half of BAV-ATAA (1.28 ± 0.03) when compared with CTRL-ATA (1.13 ± 0.02) (Fig. 5), since more undulated fibers permit increased stretch before all fibers become engaged (straightened) (Tsamis et al., 2011). Nakashima et al. (1990b), who assessed histologically the media of ATA dissecting aneurysms of type-A, reported that medial microstructure was characterized by decreased number of interlaminar elastin fibers. Furthermore, these fibers had irregular arrangement and shape. The change in microstructure was more pronounced in the outer-media. Our study revealed that elastin fibers were more structurally disorganized about the Θ-axis in the outer-media specifically of BAV-ATAA, as indicated by the lower OI when compared with CTRL-ATA (Fig. 3B). In the right-lateral region of TAV-ATAA, Sokolis et al. (2012) demonstrated that elastin fibers of the media were aligned in Z-axis in the inner layers but primarily oriented in the Θ-direction in the outer layers, as opposed to fibers oriented in both the Θ and Z-directions in the media of the other wall regions. This deviation of elastin orientation may be associated with micro-tears of elastin in the inner wall along the Θ-axis. Our data supports the notion that elastin fibers are specifically Θ-oriented, albeit less aligned in the Θ-axis, in the outer-media in BAV-ATAA but not TAV-ATAA (Fig. 3A D).

With respect to collagen micro-architecture, Sariola et al. (1986) showed that interlaminar collagen deposition was more concentrated in ATA dissection when compared with CTRL-ATA. In dissected specimens exhibiting cystic medial degeneration, collagen fibers were found to be organized as thick bundles within the media having Z-orientation. Sokolis et al. (2012) also reported that collagen fibers formed bundles about the Z-axis in the subintimal layers of the right-lateral region of TAV-ATAA. The results of our study are consistent with these findings in that collagen fibers were found to be more radially-oriented in the outer-medial layers of BAV-ATAA when compared with CTRL-ATA (Fig. 3E). Collectively, our data suggest that fiber micro-architecture differs in the various tissue planes among patients grouped by valve phenotype, and could explain our observed differences in biomechanical properties in BAV-ATAA vs. TAV-ATAA (Pasta et al., 2012; Pichamuthu et al., in press).

4.3. Association of ATAA diameter and patient age with fiber micro-architecture

As the aneurysm maximal orthogonal diameter increases, linear regression analysis revealed that collagen fibers in the inner-media of TAV-ATAA were less radially-oriented, and more

aligned and oriented in the Θ-direction. From a biomechanical standpoint, this result suggests increased stretching of the medial layer attendant with decreased fiber undulation about the Θ-axis as an aneurysm enlarges.

Moreover, our imaging analysis shows that collagen fibers are less radially-oriented and elastin fibers are more aligned in the Z-axis in the inner-media of TAV-ATAA with increasing age. This trend was similar for the inner-medial micro-architecture of elastin and collagen fibers in the Θ-RAD plane of BAV-ATAA as well, with fibers observed to be less undulated about the Θ-axis and more aligned in the Θ-axis in the inner-media with increasing age, but the correlation with age did not attain statistical significance ($p > 0.05$, results not shown). Within the outer-media of TAV-ATAA, collagen became more undulated about the Z-axis with increasing age. This discrepancy in fiber micro-architecture with fibers in inner layers being more stretched and with disrupted radially-oriented components than fibers in outer layers may contribute to distinct mechanisms mediating development, progression and vascular remodeling associated with aneurysms arising in TAV vs. BAV patients.

Looking at the elastin content in ATA disease and aging, it was observed by Phillippi et al. (in press) that the content was similar among aneurysmal and non-aneurysmal ATA with BAV or TAV. Also, it has been previously reported that the total elastin content remained unchanged in ATA dissection (Cattell et al., 1993; de Figueiredo Borges et al., 2008; Nakashima et al., 1990a; Nakashima et al., 1990b; Sariola et al., 1986; Wang et al., 2005) and in CTRL-ATA (Andreotti et al., 1985) with increasing age, but elastin concentration has been shown to be decreased in CTRL-ATA with increasing age (Halme et al., 1985; Hosoda et al., 1984; Wang et al., 2005).

With regard to collagen content in ATA disease and aging, studies have suggested that it is increased in thoracic aortic dissections (de Figueiredo Borges et al., 2008; Wang et al., 2006) and abdominal aortic aneurysms (Menashi et al., 1987; Rizzo et al., 1989), whereas no change in collagen content has been reported in ATAA and abdominal aortic aneurysms of Marfan patients (Lindeman et al., 2010) or in BAV-ATAA (Fedak et al., 2003). Looking at specific regions of ATAA, Della Corte et al. (2008) reported that collagen content is spatially-dependent in BAV-ATAA. Also, Phillippi et al. (2010) have found that the levels of type-I collagen mRNA are elevated in BAV-ATAA, and Pichamuthu et al. (in press) have observed that the total collagen content is unchanged between BAV and TAV-ATAA. According to other studies it remains unclear whether total collagen content is unchanged (Hosoda et al., 1984) or is increased as patient age increases (Andreotti et al., 1985; Halme et al., 1985). However, aging may compound micro-architectural changes in the aorta (Gleason, 2005; Tadros et al., 2009). Although the patient age and aneurysm diameter did not impact the delamination strength of aortic media (Pasta et al., 2012), it was shown by Pichamuthu et al. (in press) that when the tensile strength of BAV-ATAA was linearly extrapolated to the corresponding age of TAV-ATAA, the strength of BAV-ATAA remained higher than TAV-ATAA. These collective findings provoke the need for additional studies to further characterize the micro-architectural changes that occur in ATA including changes of the interlaminar or radially-oriented components and variation of fiber undulation about Z and Θ-axes.

4.4. Limitations

The main limitation of this study is that we characterized fiber micro-architecture in the traction-free state of BAV-ATAA, TAV-ATAA and CTRL-ATA. However, the aneurysmal diameter was measured at the deformed (loaded) state just before the surgical tissue was excised. Therefore the above-mentioned link to biomechanics would be reasonable under the assumption that the “relative” undulation of fibers about Z and Θ-axes would be maintained

between the traction-free and deformed state. A more realistic approach would be to perform microscopy imaging of tissues under in vivo stretching conditions. Also, the aortic valve morphologic phenotype may correlate with region-specific anomalies in fiber micro-architecture. Future study would include analysis in different Θ regions of ATAA to reveal region-specific alterations, which may contribute to distinct pathways of formation and progression of ATAA in TAV vs. BAV patients.

4.5. Conclusions

We conclude that for BAV-ATAA, collagen and elastin fiber micro-architecture can be characterized as radially-oriented in the outer-media when compared with CRTL-ATA. This architectural profile may explain the observed increased tensile stretch at the inflection point of Θ-strips of adventitial-medial half of BAV-ATAA when compared with CTRL-ATA. The discrepancy in fiber micro-architecture between inner and outer-media of TAV-ATAA, with fibers in the inner layers being more stretched and with disrupted radially-oriented components than fibers in the outer layers, may be associated with distinct mechanisms of vascular remodeling in the medial layers of ATAA. We further conclude that aortic diameter and patient age do not appear to affect the medial fiber micro-architecture of BAV-ATAA in the Z-RAD and Θ-RAD planes. These findings encourage more rigorous interrogation of the micro-architectural changes within ATAAs. Collectively, our hope is that a subject-specific simulation tool could be developed for enabling the prediction of aortic remodeling and disease progression. Such a tool could ultimately provide insight into the pathophysiology of aortic disease, improve risk assessment for aortic catastrophe and help guide clinical decision-making.

Supplementary Material

Refer to Web version on PubMed Central for supplementary material.

Acknowledgments

The authors would like to acknowledge funding support of this work by the Swiss National Science Foundation Fellowships for Advanced Researcher Numbers PA00P2_139684 and PA00P2_145399 (Dr. Tsamis), by the University of Pittsburgh's Swanson School of Engineering (Mr. Koch), by the Fondazione Ri.MED (Drs. D'Amore and Pasta), by the NIH R01 HL109132 (Drs. Gleason and Vorp), and by the University of Pittsburgh's Department of Cardiothoracic Surgery (Dr. Vorp). We would like to thank Mr. Michael Eskay and Mr. Benjamin Green for assistance in harvesting human ATA tissue.

References

Andreotti L, Bussotti A, Cammelli D, di Giovine F, Sampognaro S, Sterrantino G, Varcasia G, Arcangeli P. Aortic connective tissue in ageing – a biochemical study. Angiology. 1985; 36:872–879. [PubMed: 4083569]

Cahalan MD, Parker I, Wei SH, Miller MJ. Two-photon tissue imaging: seeing the immune system in a fresh light. Nature Reviews Immunology. 2002; 2:872–880.

Cattell MA, Hasleton PS, Anderson JC. Increased elastin content and decreased elastin concentration may be predisposing factors in dissecting aneurysms of human thoracic aorta. Cardiovascular Research. 1993; 27:176–181. [PubMed: 8472268]

D'Amore A, Stella JA, Wagner WR, Sacks MS. Characterization of the complete fiber network topology of planar fibrous tissues and scaffolds. Biomaterials. 2010; 31:5345–5354. [PubMed: 20398930]

de Figueiredo Borges L, Jaldin RG, Dias RR, Stolf NA, Michel JB, Gutierrez PS. Collagen is reduced and disrupted in human aneurysms and dissections of ascending aorta. Human Pathology. 2008; 39:437–443. [PubMed: 18261628]

Della Corte A, Quarto C, Bancone C, Castaldo C, Di Meglio F, Nurzynska D, De Santo LS, De Feo M, Scardone M, Montagnani S, Cotrufo M. Spatiotemporal patterns of smooth muscle cell changes in ascending aortic dilatation with bicuspid and tricuspid aortic valve stenosis: focus on cell-matrix signaling. Journal of Thoracic and Cardiovascular Surgery. 2008; 135:8–18. 18 e1-2. [PubMed: 18179910]

Fedak PW, de Sa MP, Verma S, Nili N, Kazemian P, Butany J, Strauss BH, Weisel RD, David TE. Vascular matrix remodeling in patients with bicuspid aortic valve malformations: implications for aortic dilatation. Journal of Thoracic and Cardiovascular Surgery. 2003; 126:797–806. [PubMed: 14502156]

Gleason TG. Heritable disorders predisposing to aortic dissection. Seminars in Thoracic and Cardiovascular Surgery. 2005; 17:274–281. [PubMed: 16253833]

Halme T, Savunen T, Aho H, Vihersaari T, Penttinen R. Elastin and collagen in the aortic wall: changes in the Marfan syndrome and annuloaortic ectasia. Experimental and Molecular Pathology. 1985; 43:1–12. [PubMed: 4007138]

Hosoda Y, Kawano K, Yamasawa F, Ishii T, Shibata T, Inayama S. Age-dependent changes of collagen and elastin content in human aorta and pulmonary artery. Angiology. 1984; 35:615–621. [PubMed: 6497045]

Jiang X, Zhong J, Liu Y, Yu H, Zhuo S, Chen J. Two-photon fluorescence and second-harmonic generation imaging of collagen in human tissue based on multiphoton microscopy. Scanning. 2011; 33:53–56. [PubMed: 21328394]

Jondeau G, Boileau C. Genetics of thoracic aortic aneurysms. Current Atherosclerosis Reports. 2012; 14:219–226. [PubMed: 22415348]

Karlon WJ, Covell JW, McCulloch AD, Hunter JJ, Omens JH. Automated measurement of myofiber disarray in transgenic mice with ventricular expression of ras. Anatomical Record. 1998; 252:612–625. [PubMed: 9845212]

Konig K, Schenke-Layland K, Riemann I, Stock UA. Multiphoton auto-fluorescence imaging of intratissue elastic fibers. Biomaterials. 2005; 26:495–500. [PubMed: 15276357]

Lindeman JH, Ashcroft BA, Beenakker JW, van Es M, Koekkoek NB, Prins FA, Tielemans JF, Abdul-Hussien H, Bank RA, Oosterkamp TH. Distinct defects in collagen microarchitecture underlie vessel-wall failure in advanced abdominal aneurysms and aneurysms in Marfan syndrome. Proceedings of the National Academy of Sciences of the United States of America. 2010; 107:862–865. [PubMed: 20080766]

Lu S, Sun X, Hong T, Yang S, Song K, Lai H, Hu K, Wang C. Bilateral versus unilateral antegrade cerebral perfusion in arch reconstruction for aortic dissection. Annals of Thoracic Surgery. 2012; 93:1917–1920. [PubMed: 22560261]

Masuda Y, Yamada Z, Morooka N, Watanabe S, Inagaki Y. Prognosis of patients with medically treated aortic dissections. Circulation. 1991; 84(III):7–13.

Matsushita A, Manabe S, Tabata M, Fukui T, Shimokawa T, Takanashi S. Efficacy and pitfalls of transapical cannulation for the repair of acute type A aortic dissection. Annals of Thoracic Surgery. 2012; 93:1905–1909. [PubMed: 22483651]

Menashi S, Campa JS, Greenhalgh RM, Powell JT. Collagen in abdominal aortic aneurysm: typing, content, and degradation. Journal of Vascular Surgery. 1987; 6:578–582. [PubMed: 2826827]

Nakashima Y, Kurozumi T, Sueishi K, Tanaka K. Dissecting aneurysm: a clinicopathologic and histopathologic study of 111 autopsied cases. Human Pathology. 1990a; 21:291–296. [PubMed: 2312107]

Nakashima Y, Shiokawa Y, Sueishi K. Alterations of elastic architecture in human aortic dissecting aneurysm. Laboratory Investigation. 1990b; 62:751–760. [PubMed: 2359259]

Pasta S, Phillippi JA, Gleason TG, Vorp DA. Effect of aneurysm on the mechanical dissection properties of the human ascending thoracic aorta. Journal of Thoracic and Cardiovascular Surgery. 2012; 143:460–467. [PubMed: 21868041]

Phillippi JA, Eskay MA, Kubala AA, Pitt BR, Gleason TG. Altered oxidative stress responses and increased type I collagen expression in bicuspid aortic valve patients. The Annals of Thoracic Surgery. 2010; 90:1893–1898. [PubMed: 21095332]

Phillippi, JA.; Green, BR.; Eskay, MA.; Hill, MR.; Robertson, AM.; Vorp, DA.; Gleason, TG. Mechanism of aortic medial matrix remodeling is distinct in bicuspid aortic valve patients. Journal of Thoracic and Cardiovascular Surgery. 2013. http://dx.doi.org/10.1016/j.jtcvs.2013.04.028, in press

Pichamuthu, JE.; Phillippi, JA.; Cleary, DA.; Chew, DW.; Hempel, J.; Vorp, DA.; Gleason, TG. Differential tensile strength and collagen composition in ascending aortic aneurysms by aortic valve phenotype. Annals of Thoracic Surgery. 2013. http://dx.doi.org/10.1016/j.athoracsur.2013.07.001, in press

Rizzo RJ, McCarthy WJ, Dixit SN, Lilly MP, Shively VP, Flinn WR, Yao JS. Collagen types and matrix protein content in human abdominal aortic aneurysms. Journal of Vascular Surgery. 1989; 10:365–373. [PubMed: 2795760]

Sariola H, Viljanen T, Luosto R. Histological pattern and changes in extracellular matrix in aortic dissections. Journal of Clinical Pathology. 1986; 39:1074–1081. [PubMed: 3537014]

Sokolis DP, Kritharis EP, Giagini AT, Lampropoulos KM, Papadodima SA, Iliopoulos DC. Biomechanical response of ascending thoracic aortic aneurysms: association with structural remodelling. Computer Methods in Biomechanics and Biomedical Engineering. 2012; 15:231–248. [PubMed: 21480082]

Tadros TM, Klein MD, Shapira OM. Ascending aortic dilatation associated with bicuspid aortic valve pathophysiology, molecular biology, and clinical implications. Circulation. 2009; 119:880–890. [PubMed: 19221231]

Takigawa M, Yoshimuta T, Akutsu K, Takeshita S, Yokoyama N. Prevalence and predictors of coexistent silent atherosclerotic cardiovascular disease in patients with abdominal aortic aneurysm without previous symptomatic cardiovascular diseases. Angiology. 2012; 63:380–385. [PubMed: 21948971]

Tsamis A, Rachev A, Stergiopulos N. A constituent-based model of age-related changes in conduit arteries. American Journal of Physiology – Heart Circulatory Physiology. 2011; 301:H1286–H1301. [PubMed: 21724865]

Wang X, LeMaire SA, Chen L, Carter SA, Shen YH, Gan Y, Bartsch H, Wilks JA, Utama B, Ou H, Thompson RW, Coselli JS, Wang XL. Decreased expression of fibulin-5 correlates with reduced elastin in thoracic aortic dissection. Surgery. 2005; 138:352–359. [PubMed: 16153447]

Wang X, LeMaire SA, Chen L, Shen YH, Gan Y, Bartsch H, Carter SA, Utama B, Ou H, Coselli JS, Wang XL. Increased collagen deposition and elevated expression of connective tissue growth factor in human thoracic aortic dissection. Circulation. 2006; 114:I200–I205. [PubMed: 16820572]

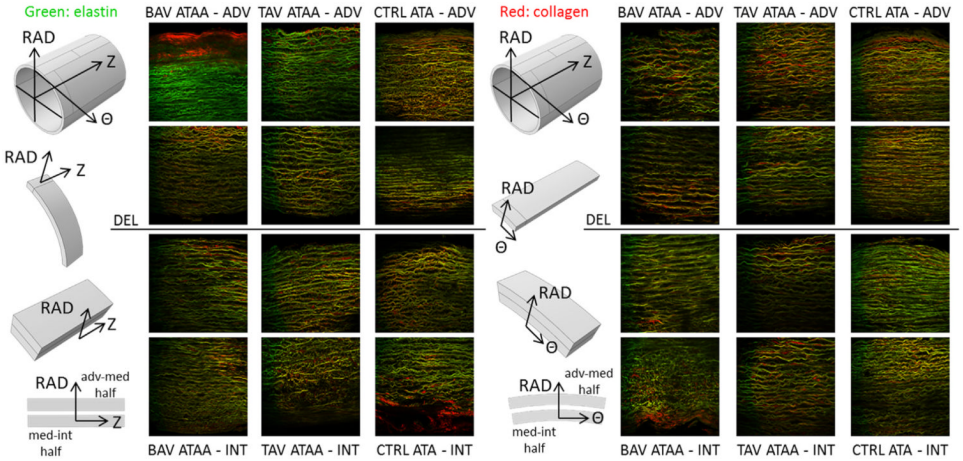

Fig. 1.

Example full wall thickness multi-photon microscopy images (0. 5 × 0.5 mm^2 each) of elastin (green) and collagen (red) fibers in the *Z*-RAD (columns 2-4) and *Θ*-RAD planes (columns 6-8) of BAV-ATAA (columns 2,6), TAV-ATAA (columns 3,7) and CTRL-ATA (columns 4,8). Column 1: The adventitial-medial and medial-intimal delaminated halves from *Θ* strips were placed under the microscope with the Z-RAD plane facing up. Column 4: The adventitial-medial and medial-intimal delaminated halves from Z strips were placed under the microscope with the *Θ*-RAD plane facing up. Rows 1,2: The adventitial-medial delaminated half. Rows 3,4: The medial-intimal delaminated half.

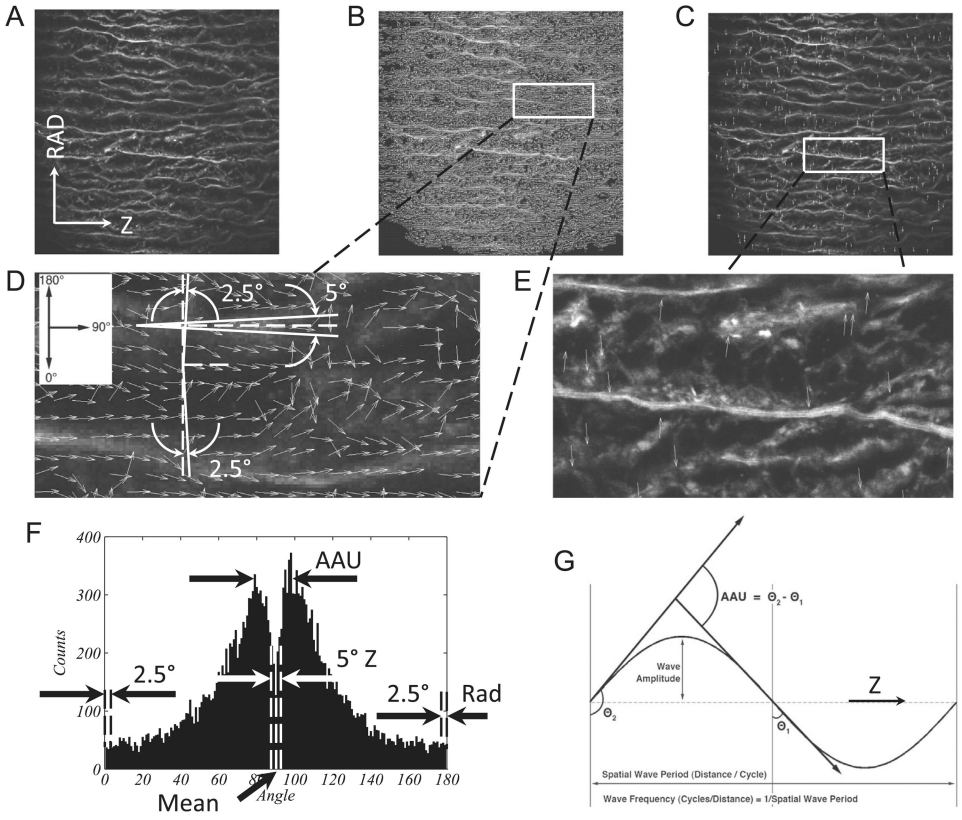

Fig. 2.

(A) Representative multi-photon microscopy image (0.5 × 0.5 mm^2) of collagen fibers in the outer media of TAV-ATAA in the Z-RAD plane. The border of dissected medial surface is on the bottom. (B) Processed image with small arrows in white that follow the direction of the fibers. (C) Processed image with the radially-oriented fiber segments overlaid in white color. (D) A higher magnification of a small area of (B). (D) also shows how the script filters the fiber components that have a Z or RAD orientation using a small angle tolerance of 5°. Since the angle of orientation cannot be higher than 180° or lower than 0°, the tolerance of 5° for the radially-oriented components is split in 2.5° for those pointing downward and 2.5° for those pointing upward. (E) A higher magnification of a small area of (C). (F) Number distribution of the orientation angle of all the small fiber segments. The histogram provides the mean angle of orientation and also is characteristic of two peaks. The angle difference between the two peaks represents the average amplitude of angular undulation (AAU) of the fibers. Figure F also indicates the parts of the histogram that correspond to fibers oriented in the Z or RAD direction. (G) Graphical explanation of AAU. A fiber is shown to undulate between a minimum angle θ_1 and a maximum angle θ_2. The difference between the two angles is equal to AAU. The output of the automated image-based analysis tool for the particular case of Fig. 2A is: RAD%=1.96%, *Z*% =12.65%, RAD/Z=0.16, mean angle=89°, amplitude of angular undulation=15°, and *OI*=0.73 with respect to the mean angle.

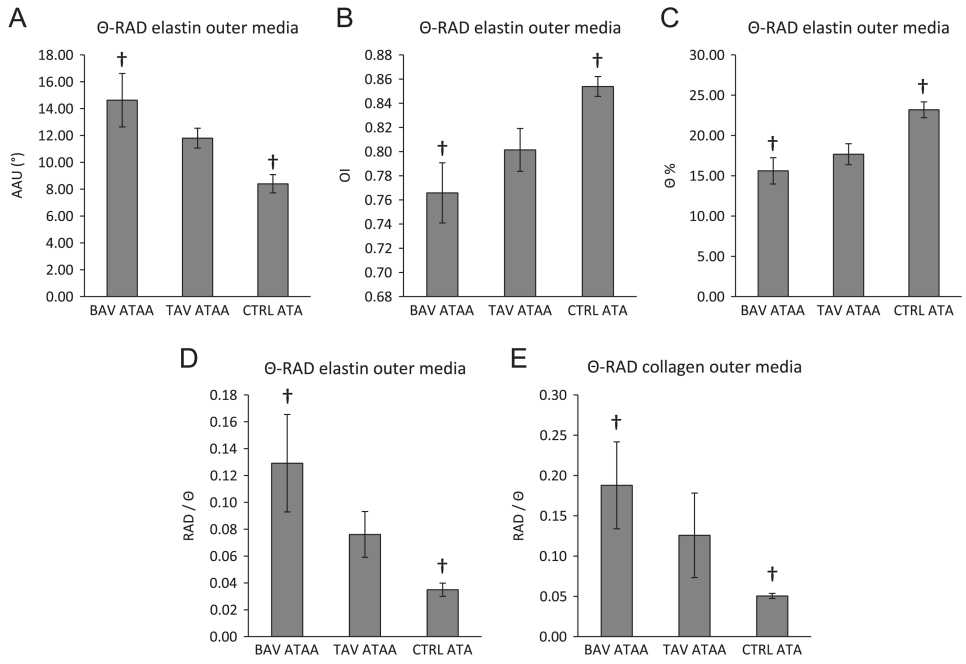

Fig. 3.

Results of ANOVA analysis to determine the significant differences ($p<0.05$) in the collagen and elastin micro-architecture among the three aortic phenotypes in the outer media of the Θ-RAD plane based on the output of the custom MATLAB written automated image-based analysis tool. Results are presented as mean ± standard error of the mean. † indicates significant differences. (A) Amplitude of angular undulation of elastin in the outer media in the Θ-RAD plane, (B) Orientation index of elastin in the outer media in the Θ-RAD plane, (C) Percentage of elastin fibers oriented in the Θ direction in the outer media in the Θ-RAD plane, (D) Ratio of elastin fibers oriented in the RAD direction over elastin fibers oriented in the Θ direction in the outer media in the Θ-RAD plane, (E) Ratio of collagen fibers oriented in the RAD direction over collagen fibers oriented in the Θ direction in the outer media in the Θ-RAD plane.

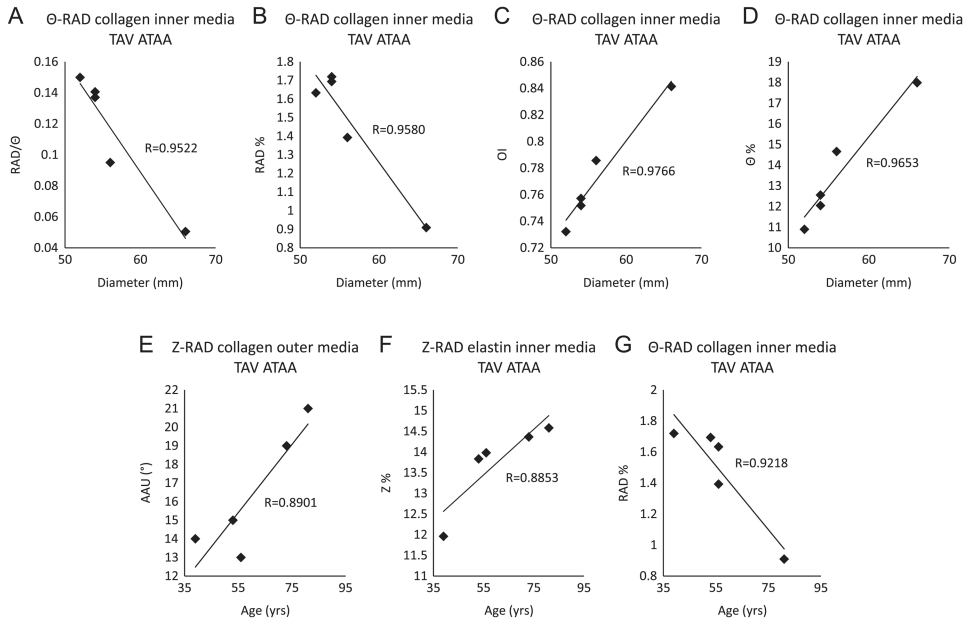

Fig. 4.

Results of linear regression analysis to reveal statistically significant correlations ($p<0.05$) of micro-architectural parameters with aneurysm diameter and patient age. (A) Ratio of collagen fibers oriented in the RAD direction over collagen fibers oriented in the Θ direction as a function of diameter in the inner media in the Θ-RAD plane of TAV-ATAA, (B) Percentage of collagen fibers oriented in the RAD direction as a function of diameter in the inner media in the Θ-RAD plane of TAV-ATAA, (C) Orientation index of collagen fibers as a function of diameter in the inner media in the Θ-RAD plane of TAV-ATAA, (D) Percentage of collagen fibers oriented in the Θ direction as a function of diameter in the inner media in the Θ-RAD plane of TAV-ATAA, (E) Amplitude of angular undulation of collagen fibers as a function of age in the outer media in the Z-RAD plane of TAV-ATAA, (F) Percentage of elastin fibers oriented in the Z-direction as a function of age in the inner media in the Z-RAD plane of TAV-ATAA, (G) Percentage of collagen fibers oriented in the RAD direction as a function of age in the inner media in the Θ-RAD plane of TAV-ATAA.

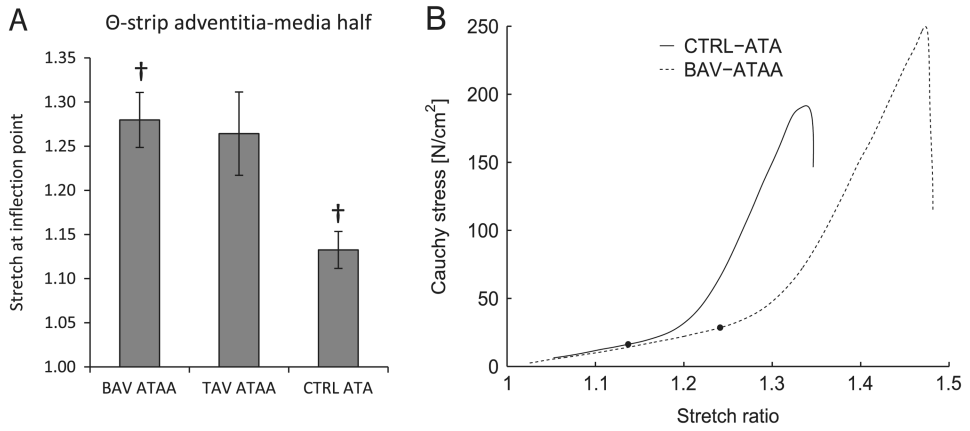

Fig. 5.

Θ-strips of adventitia-media halves of BAV-ATAA, TAV-ATAA and CTRL-ATA were subjected to tensile testing (Pasta et al., 2012). A subset of the tensile stress-stretch curves of the original study (BAV-ATAA, n=7; TAV-ATAA, n=3; CTRL-ATA, n=4) were analyzed in the current study to calculate the stretch at the inflection point, corresponding to the stretch at which the second derivative of the curve becomes positive. (A) Results of ANOVA analysis (One-way, Tukey post-hoc test for unequal samples) using SigmaPlot software (SYSTAT Software, Chicago, Ill) to determine the significant differences (p<0.05) in the stretch at inflection point among the three aortic phenotypes. It was found that the tensile stretch at the inflection point for BAV-ATAA (1.28 ± 0.03) was higher than CTRL-ATA (1.13 ± 0.02). Results are presented as mean ± standard error of the mean.† indicates significant differences. (B) Representative Cauchy stress-stretch curves for adventitia-media half of *Θ*-strip of CTRL-ATA (solid line) and BAV-ATAA (dashed line). The black circular markers on the stress-stretch curves indicate the location of the inflection points.

Table 1

Clinical data of patients for aortic tissue used for multi-photon microscopy.

All Samples	N (M/F)	Age, yr (Median ± S.D.)	Aortic dia., mm (Mean ± S.D.)	HTN (%)	Smoking (%)	AI (%)			AS (%)		
						1+	2–3+	4+	Mild	Moderate	Severe
CTRL ATA	5 (2/3)	58 ± 4.7	Normal	40	40	0	0	20	0	0	0
TAV ATAA	5(3/2)	67 ± 11.7	56.4 ± 5.55	80	0	40	40	20	0	0	0
BAV ATAA	8 (6/2)	60 ± 8.7	53.8 ± 8.38	25	25	25	0	25	0	0	12.5

N, number; *M*, male; F, female; S.D., standard deviation; Dia., diameter; BAV, bicuspid aortic valve; TAV, tricuspid aortic valve; CTRL, control; ATA, ascending thoracic aorta; ATAA, ascending thoracic aortic aneurysm; HTN, hypertension; AI, aortic insufficiency; AS, aortic stenosis.